Structural and Morphological Characterization by Energy Dispersive X-ray Diffractometry and Reflectometry Measurements of Cr/Pt Bilayer Films

Barbara Paci,*,† Amanda Generosi,† Valerio Rossi Albertini,† Elisabetta Agostinelli,‡ Gaspare Varvaro,‡ and Dino Fiorani‡

Istituto di Struttura della Materia, Consiglio Nazionale delle Ricerche, Area di Ricerca di Tor Vergata, Via del Fosso del Cavaliere 100, 00133 Roma, Italy, and Istituto di Struttura della Materia, Consiglio Nazionale delle Ricerche, Area di Ricerca di Montelibretti, Via Salaria km 29.500, 00016 Monterotondo Scalo, Italy

Received June 24, 2003. Revised Manuscript Received October 30, 2003

The characteristics of Cr thin films, currently used as resistors, as capacitor plates, and in magnetic recording hard disks, strongly depend on the deposition modality. Nevertheless, up to date no systematic study of the influence of the deposition conditions and of the substrate used on the films structural and morphological properties has been carried out. In the present work, the energy dispersive X-ray diffraction and reflectometry (EDXD and EDXR) techniques were used to investigate double-layer Cr/Pt thin films, deposited by pulsed laser deposition (PLD) at different temperatures (from RT to 600 °C) both on crystalline (Si and MgO) and on amorphous (SiO_2) substrates. The synergy of the two X-ray techniques allows correlating the structural properties of the samples (obtained by the EDXD) to their morphological characteristics (provided by EDXR). The result is that when the PLD deposition is performed under suitable working conditions and with use of crystalline substrates, films with good texture and with very smooth surfaces were obtained, as required by the magnetorecording applications. Moreover, the structural quality appears to be independent of the deposition temperature. Finally, the advantages connected with the joint use of the energy-dispersive X-ray diffraction and reflectometry are shortly discussed.

1. Introduction

Chromium thin films are routinely used for a number of applications, in integrated circuits, photomasks, and optical beam splitters and as underlayers in multilayered magnetic media for high-density magnetorecording.[1] The Cr film, in the last case, acts as a structural template for inducing the epitaxial growth of the magnetic Co-based film.[2,3] A crucial step to improving the magnetic and recording characteristics of multilayer media is the understanding of the inter-relationship between the deposition processes and the resulting microstructural properties of the film. In hard disk fabrication sputtering[4] deposition is the most commonly used technique. However, it has recently been shown[5] that higher adatom mobility is beneficial in improving the magnetic performances and reliability of thin film magnetic media since it reduces the final pinhole density. Other film deposition techniques, like pulsed laser deposition (PLD), usually produce films with higher crystalline quality in comparison with those obtained by sputtering, one of the main reasons being the higher kinetic energy of the species emitted in the plasma (keV for ions, several eV for neutrals, when the energy fluence is of the order of 10^8-10^9 W/cm^2). In such conditions, indeed, higher adatom mobility is usually obtained. Furthermore, in the PLD process nuclei with small size are produced, due to the high level of supersaturation. This results in a two-dimensional nucleation of mono-atomic height, favorable to the “layer growth” of the films. For this reason, films with improved surface morphology can be produced.

In the present work, the structural and morphological study of a series of PLD high-quality double-layer Cr/Pt thin films, by means of the energy dispersive X-ray diffraction and reflectometry techniques[6−10] is presented. In particular, from the EDXR, an accurate determination of the films thickness and roughness is given, while from the EDXD measurements both the lattice parameters and the rocking curves of the major

* To whom correspondence should be addressed. E-mail: barbara.paci@ism.rm.cnr.it.
† Consiglio Nazionale delle Ricerche, Area di Ricerca di Tor Vergata.
‡ Consiglio Nazionale delle Ricerche, Area di Ricerca di Montelibretti.

(1) Lambeth, D. N. In *Magnetic Storage System Beyond 2000*; Hadjipanayis, G. C., Ed.; Kluwer Academic Publishers: Dordrecht, 2001; pp 55−74.
(2) Choe, G.; Chung, S. J.; Walser, R. M. *Thin Solid Films* **1995**, *259*, 231.
(3) Laughlin, D. E.; Feng, Y. C.; Lambeth, D. N.; Lee, L.-L.; Tang, L. *JMMM* **1996**, *155*, 146.
(4) Chia, R. W. J.; Wang, C. C.; Lee, J. J. K. *J. Magn. Magn. Mater.* **2000**, *209*, 45.
(5) Laughlin, D. E.; Feng, Y. C.; Lambeth, D. N. *J. Appl. Phys.* **1994**, *76*, 7311.
(6) Giessen, B. C.; Gordon, G. E. *Science* **1968**, *159*, 973.
(7) Nishikawa, K.; Iijima, T. *Bull. Chem. Soc. Jpn.* **1984**, *57*, 1750.
(8) Roser, S. J.; Felici R.; Eaglesham, A. *Langmuir* **1994**, *10*, 3853.
(9) Matsubara, E.; Sato, S.; Imafuku, M.; Nakamura, T.; Koshiba, H.; Inoue A.; Waseda, Y. *Mater. Trans., JIM* **2000**, *41*, 11, 1379.
(10) Park, C.; Saito, M.; Waseda, Y.; Nishiyama, N.; Inoue, A. *Mater. Trans., JIM* **1999**, *40*, 491.

10.1021/cm031100h CCC: $27.50
Published on Web 12/25/2003

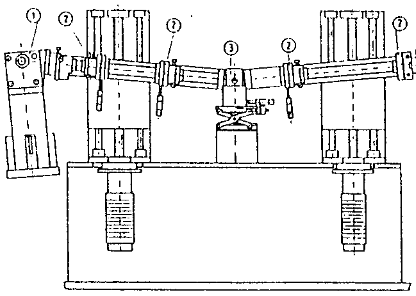

Figure 1. Sketch of the energy-dispersive X-ray diffractometer. The fundamental components are as follows: (1) X-ray source (W anode tube), (2) collimation slits, (3) sample holder, and (4) Ge single-crystal energy-sensitive detector.

Bragg peaks are obtained, allowing one to precisely evaluate the film degree of epitaxy. To perform the X-ray diffractometry or reflectometry measurements using the energy dispersive technique (ED), the sample is irradiated by a continuous spectrum X-ray beam, defined as "white". The energy spectrum of the radiation after interaction with the sample (i.e., scattered or reflected, respectively) is acquired by an energy-sensitive detector. One major merit of the ED techniques, compared to the conventional angular-dispersive (AD) one, is that the experimental set-up is static, no motion of the diffractometer arms being needed. When reflection geometry has to be used, this characteristic guarantees that the irradiated part of the sample surface is unchanged during the collection time. Moreover, at a parity of statistical accuracy, the time saving is about 1 order of magnitude, corresponding to the ratio between the number of photons concentrated in the fluorescence line (primary beam in AD) and the number of photons distributed along the white spectrum.

In the EDXD, the whole pattern is obtained in a single measurement, providing a fast recording of film Bragg peaks and, consequently, of their rocking curves, as well as of the reflectivity spectra. This is particularly important when thin films are analyzed since the scarceness of the material available for the scattering may make the measurements of diffraction patterns with acceptable signal-to-noise ratio difficult and time-consuming. Finally, when an X-ray reflectivity measurement of a thin film is performed, the decrease in q resolution due to the uncertainties on both the angle and the energy, which is the main drawback of the ED technique, does not remarkably affect the reflectometry spectra, which are characterized by broad peaks or long period of oscillations.

2. Experimental Section

2.1. Samples. The films were deposited by PLD using a Lambda Physik excimer laser ArF ($\lambda = 193$ nm) at an energy fluence of 5 J/cm^2 and a pulse repetition rate of 10 Hz. Deposition was performed on nonetched Si(100), MgO(100), and amorphous SiO_2 substrates in a frontal geometry, with 4-cm distance between target and substrate at various temperatures. A HV chamber with a liquid nitrogen trap ($P_{\mathrm{back}} = 7 \times 10^{-8}$ mbar; $P_{\mathrm{growth}} = 2 \times 10^{-7}$ mbar) was used. Films were deposited at temperatures ranging from 25 to 600 °C. A carousel with metallic Cr and Pt targets was used to sequentially deposit the two different layers.

2.2. Diffractometer-Reflectometer. The energy-dispersive diffractometer-reflectometer is shown in Figure 1. It consists of a noncommercial instrument equipped with a water-cooled X-ray W anode tube (Philips, model PW2214/20) supplied at 58 kV and 30 mA. The white beam is collimated by two W slits and reaches the sample placed in the center of rotation of the machine arms. The two slits of the second arm select the portion of the diffracted beam contained in the acceptance angle of the detector, which is an EG&G ultrapure Ge solid-state detector (SSD), cooled by a liquid nitrogen bath and connected to an integrated spectroscopy amplifier-multichannel analyzer system (92 x spectrum master).

2.3. Experimental Methods. The experimental set-up described above is used to perform combined energy-dispersive X-ray reflectometry and diffractometry measurements, allowing the investigation of both the morphological and the structural properties of the films under study. The only relevant difference between the instrumental configurations used in the two kinds of measurements, both performed in the reflection geometry, is the order of magnitude of the deflection angle, that is, the q-range scanned during the data acquisition.

2.3.1. X-ray Reflectometry Measurements. The X-ray reflectometry technique is sensitive to surfaces and interfaces morphology at the Angstrom resolution.

If the incidence and reflection angles are measured referring to the sample surface, Snell law reads: $n_1 \cos\theta_1 = n_2 \cos\theta_2$. In the case the sample is in air, there is a value of θ_1, called critical angle θ_c, at which $\cos\theta_c = n_2(n_{\mathrm{air}} = 1)$. In these conditions, the beam will not be refracted any more, but totally reflected. The general expression of the complex refractive index for X-rays is $n = 1 - (\lambda^2/2\pi)\rho r_0 Z^2 + i(\lambda/4\pi)\mu$, where λ is the incident wavelength, ρ is the material density, r_0 is the classical electron radius, Z is the atomic number, and μ is the linear absorption coefficient. The imaginary component, responsible for absorption, is of the order of 10^{-7} Å and, in the present case, can be neglected[11]in the calculation. This assumption may not be valid when the beam energy is close to the absorption edge, if the film is very thick or made of heavy atoms. In these cases the contribution of the imaginary part should be accounted for. The Snell law for an incident X-ray beam becomes $\cos\theta_c = 1 - \rho\lambda^2 r_0 Z^2/2\pi$. Since the values of θ_c are very small, this expression can be developed in McLaureen powers, leading to the total reflection condition for X-rays: $(\theta_c/\lambda) = Z(\rho r_0/2)^{1/2}$ = constant. Since at the second-order approximation $\theta/\lambda \approx \sin\theta/\lambda$, it corresponds to the momentum transfer q. Therefore, a more proper way to describe the reflectivity spectra is to express the reflected intensity as a function of q. When $q < q_c$, the X-ray radiation impinging on the sample is totally reflected while when $q \approx q_c$, the radiation starts penetrating the sample and as soon as $q > q_c$, the reflectivity decays more than exponentially. The position of the critical edge ($q = q_c$) and the reflectivity profile of the threshold are determined by the material density and the surface roughness (defined as the variance from the average thickness), respectively.

In the case an X-ray beam impinges a film deposited on a substrate, it is partially reflected at the two interfaces (air–film and film–substrate) and the two reflected components interfere, producing an almost sinusoidal modulation of the reflectivity. The period of the modulation is connected to the film thickness, while the inclination of the threshold and the damping of the oscillations are related to both the surface and the interface roughness. Once the normalization of the collected spectra with respect to the spectral distribution of the incident beam is accomplished, the following model for the reflectivity of a film on a substrate[12] is used to fit the experimental data,

$$|R|^2 = \{1 - 2[Re(R_1{}^*R_r - R_1R_r)\exp(-qD)]/[1 + \exp(-2qD) - 2Re(R_1R_r)\exp(-qD)] \quad (1)$$

where $R_1 = (k_0 - k_f)/(k_0 + k_f)$ and $R_r = (k_f - k_s)/(k_f + k_s)$ are the film and substrate reflectivities, which are functions of the wavenumber in the air (k_0), in the film (k_f), and in the substrate

(11) Felici, R. *Rigaku J.* **1995**, *12*, 1.
(12) Parratt, L. G. *Phys. Rev.* **1954**, *95*, 359.

(k_s) and D is the film average thickness. When the film surface or the film−substrate interface are not sharp, the reflected intensity is modified by a roughness term similar to a Debye-Waller factor.[13]

2.3.2. X-ray Diffractometry Measurements. The rocking curve of a polycrystal represents the statistical distribution of the domains orientation. It can be measured by recording the intensity of the diffracted radiation as a function of an asymmetry parameter $\alpha = (\vartheta_i - \vartheta_f)/2$, where ϑ_i and ϑ_f are the initial (incidence) and final (deflection) angles and $\vartheta_i + \vartheta_f = 2\vartheta$ is kept unchanged.

In the case of a multilayer film deposited on a crystalline substrate, the EDXD technique provides the simultaneous measure of all the rocking curves of the most intense Bragg reflections of each layer. In general, the distribution of the films and substrate reflection intensities, as a function of α, will be different and both a film/substrate miscut and a larger mosaic spread of the film is expected.

After the sample is placed in the center of the diffractometer, the experimental procedure consists in performing an α-scan, at a fixed 2ϑ, until the maximum diffracted intensity is reached. This maximum intensity is due to the substrate reflections since the ratio between the film and the substrate thickness is several orders of magnitude. We assume the symmetry condition for the substrate as the reference position ($\alpha = 0°$).

The film reflections are expected to have the maximum intensity close to the reference position since the film tends to grow with its *c*-axis approximately perpendicular to the substrate lattice planes.

After this preliminary set-up, an α-scan is performed at constant 2ϑ by carrying out a sequence of diffraction measurements, progressively increasing α . The scan is started from a value at which the diffracted intensity is very low (typically $\alpha = -1.5°$), and then α is increased by steps of 0.05°, until the opposite position is reached ($\alpha = 1.5°$). In the small-angle approximation, the q space is well-defined by the coordinates $q_x = \alpha E$ and $q_z = (\vartheta_i + \vartheta_f)E/2$. Since during the α-scan (q_x scan) 2ϑ is kept constant, q does not change (see Figure 2). After the diffraction data are processed (see next paragraph), the curves of the peaks intensities as a function of α can be plotted. As a result, so many rocking curves as the number of Bragg peaks visible in each diffraction pattern are simultaneously obtained.

3. Experimental Results

The aim of the present work is a systematic study of the structure and morphology of Cr/Pt bilayer films as a function of the PLD deposition parameters and of the substrate used. The results, summarized in Table 1, show that all the films deposited on crystalline substrates showed a high degree of epitaxial growth both at low and at high temperature. On the contrary, when deposition is performed on the amorphous SiO_2 substrate, the film growth is not epitaxial.

3.1. X-ray Reflectometry Measurements. We performed the fit of the reflectivity spectra using five free parameters, one to normalize the observed intensities and the others to obtain morphological, that is, film average thickness and roughness, and chemical information. The electron densities are used as free parameters, despite in this case they are known, to verify the accuracy of the fit. The relative thickness D and roughness S of the Cr and the Pt films change along the series of the investigated samples so that the reflectometry spectra will be characterized by different shapes and modulations.

(13) Sinha, S. K.; Sirota, E. B.; Garoff, S.; Stanley, H. B. *Phys. Rev. B: Condens. Matter. Mater. Phys.* **1988**, *38*, 2297.

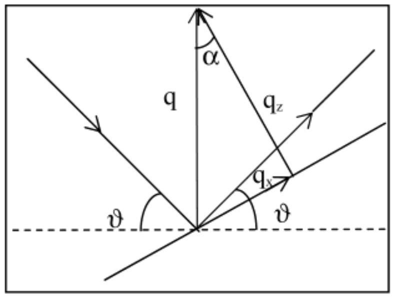

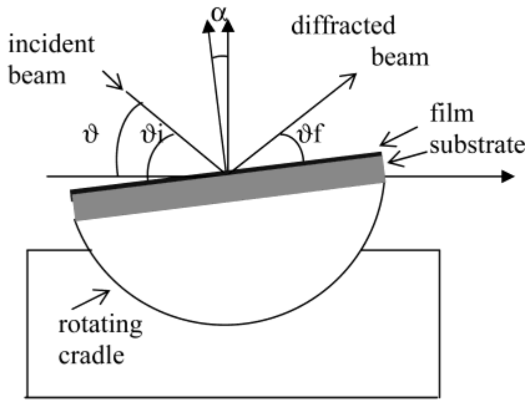

Figure 2. Scheme of the geometric set-up: the films are positioned on a cradle placed in the center of rotation of the diffractometer. The measurements are performed by rotating the cradle, that is, for different values of the asymmetry parameter $\alpha = (\vartheta_i - \vartheta_f)/2$, keeping the diffraction angle 2ϑ unchanged. In the view, the angle of rotation of the cradle is emphasized ($\alpha = 7°$), as well as film thickness, to improve the visibility.

Samples Deposited on Si and on MgO Crystalline Substrates. The reflectivity profiles of the samples deposited on Si and on MgO substrates, respectively, are shown in Figure 3 and in Figure 4 in semilog graphs together with their fits (see Table 1). The result is that for all the samples deposited on MgO and Si crystalline substrates, the Cr film roughness is below the threshold value of 6 Å. On the basis of Table 1, some preliminary observations can be made to obtain an idea of the overall characteristics of the samples. For all the samples, with the exception of samples 1 and 10, the Pt film thickness is very low (namely, around 20 Å) and its roughness is estimated to be atomically flat (namely, below 2 Å). In the cases of samples 1 and 10, the X-ray reflectivity profiles do not show the modulation produced by the interference of the two reflected beams, probably because the Pt cup layer is too thin (and/or the deposition was imperfect), to prevent the oxidation of the Cr film. This results in a very rough surface that induces a strong damping of the reflectivity signal. In this case, no information can be given on the films thickness.

It is worth noting that, in several samples, a double modulation of the spectra is visible, which is due to both the contributions of the Pt and of the Cr. To perform an acceptable fit of the data, several oscillations are required. The cup layer being rather thin, only half of the first oscillation related to it is visible.

Since the thickness of the Pt layer is not a crucial parameter, for these samples it has been estimated by a Gaussian fit of the broad oscillation present in the reflectivity spectrum and the Cr average thickness has

Table 1. Summary of the EDXD and EDXR Data Analysis for the Samples Deposited on Crystalline Substrates[a]

Pt/Cr/Si	a_0 [0.001 degree]	FWHM [0.001 degree]	D_{Pt}/D_{Cr} [Å]	S_{Pt}/S_{Cr} [Å]
sample 1 ($T = 500$ °C)	18 ± 1	50 ± 2	X-ray reflection from the surface, only	
sample 2 ($T = 400$ °C)	6 ± 1	30 ± 1	$D_{Pt} = 30 \pm 2$	$S_{Pt} < 2$
sample 3 ($T = 300$ °C)	18 ± 1	32 ± 1	$D_{Pt} = 20 \pm 2$	$S_{Cr} = 4 \pm 2$
			$D_{Cr} = 236 \pm 3$	
sample 4 ($T = 200$ °C)		Ag impurities: Cr film grown not epitaxially		
sample 5 ($T = 100$ °C)			$D_{Pt} = 72 \pm 2$	$S_{Pt} = 2 \pm 2$
sample 6 (RT)	16 ± 2	60 ± 5	$D_{Pt} = 24 \pm 2$	$S_{Cr} < 2$
			$D_{Cr} = 210 \pm 3$	

Pt/Cr/MgO	α_0 [0.001 degree]	FWHM [0.001 degree]	D_{Pt}/D_{Cr} [Å]	S_{Pt}/S_{Cr} [Å]
sample 7 ($T = 600$ °C)			$D_{Cr} = 283 \pm 3$	$S_{Cr} = 6 \pm 2$
sample 8 ($T = 500$ °C)	3 ± 2	150 ± 5	$D_{Pt} = 20 \pm 2$	$S_{Cr} < 2$
			$D_{Cr} = 500 \pm 3$	
sample 9 ($T = 400$ °C)			$D_{Pt} = 49 \pm 2$	$S_{Cr} < 2$
			$D_{Cr} = 499 \pm 3$	
sample 10 ($T = 100$ °C)			X-ray reflection from the surface, only	

[a] The results of the rocking curves analysis of the EDXD data are reported. The maxima of the rocking curves (α_0) of the Cr film do not coincide with the reference value, but are slightly misplaced. The mean value of fit FWHM gives the estimation of the epitaxy index. Thickness D and roughness S of the Pt and Cr films obtained by EDXR are reported.

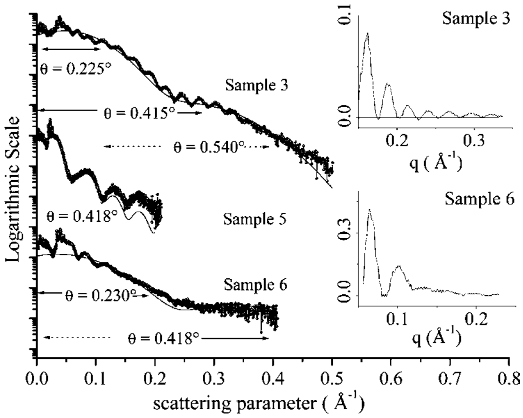

Figure 3. EDXR samples on Si: experimental data and fits. The insert shows the reflectometry spectra when the Pt contribution is subtracted: the damping of the signal gives the information needed for the computation of the film roughness S. For sample 3 the spectrum collected at $\vartheta = 0.415°$ is reported, starting from the third oscillation, that is, only the region of interest for the calculation of S.

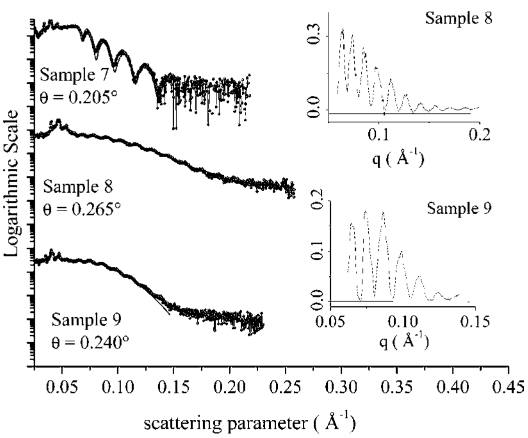

Figure 4. EDXR samples on MgO: experimental data and fits. The reflectometry spectra subtracted by the Pt contribution are reported in the insert: the range of the oscillations and relative damping is very small (although visible in the graphic), giving a film roughness below 2 Å.

been calculated by the simplified formula valid for large q values:[14] $D = \Delta q/2\pi$. Once the Pt film contribution to the signal is subtracted, the analysis of the oscillations dumping provides the values of the Cr film roughness. In any case, due to the high Pt refraction index, the Pt cap layer thickness (D_{Pt}) must be much lower than that of the Cr film (D_{Cr}); otherwise, the Cr contribution would not be visible in the reflection spectrum. The reflectometry spectrum of sample 4 is strongly affected by the presence of the Ag absorption threshold at about 25 keV, as shown in the insert of Figure 8. As will be shown in the next section, this is confirmed by the diffraction results and strongly compromises the film degree of epitaxy.

Moreover, the only sample deposited on MgO that does not show an atomically flat roughness, namely, sample 7, is about 40% thinner with respect to the other ones deposited on the same substrate: this is unexpected and indicates that the deposition process was anomalous. In the following section, we will discuss the results of the rocking curves analysis: the information given confirms this hypothesis.

3.2. X-ray Diffractometry Measurements. The rocking curves are calculated as the ratio between the intensity of a Bragg peak in correspondence of a generic α with respect to the maximum intensity of the same peak during the α-scan. In EDXD, the rocking curves of all the peaks are collected simultaneously and their calculation is not complex as in the case of a single diffraction measurement. Indeed, all the phenomena that contribute to the modification of a single EDXD diffraction pattern (spectral distribution of the primary beam, energy-dependent X-ray absorption, Compton scattering contribution) are practically unchanged during the α-scan.

The peaks of each pattern are fitted using the sum of Gaussian and linear functions: the Gaussian component takes into account the convolution of the Bragg peak with the diffractometer transport function while the linear one takes into account the contribution of an almost flat background and of the smooth Compton profile. The Gaussian integral is proportional to the peak coherent scattered intensity, which is used to

(14) Zhou, X. L.; Chen, S. H. *Theor. Found. X-ray Neutron Reflectom.*, *Phys. Rep.* **1995**, *257*, 223−348.
(15) Batchelder D. N.; Simmons R. O. J. *Chem. Phys.* **1964**, *180*, 2332.
(16) Caminiti, R.; Rossi, A. V. *Int. Rev. Phys. Chem* **1999**, *18*, 263.

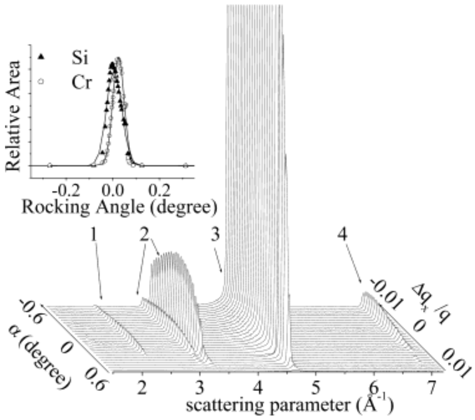

Figure 5. Sequence of the EDXD patterns for the sample no. 1 acquired during the α-scan. The peak at $q = 2.358(4)$ Å^{-1} is the (200) Si reflection. The peak at $q = 4.637(4)$ Å^{-1} , see ref 15, is the (400) reflection of Si (3), while the peaks (2) visible in the (3.096(4) Å^{-1}, 3.255(4) Å^{-1}) range are produced by the escape effect of the Ge sensitive crystal.[16] The reflection at $q = 6.978(4)$ Å^{-1} is the (310) of Cr (4). The insert reports the rocking curve; the relative area of the Cr peak is re-scaled of a factor 200 for clarity.

calculate the rocking curve, while its maximum indicates the position of the Bragg peak, required to obtain the interplanar spacing along the *c*-axis.

Since the X-ray diffraction provides information about the lattice structure in the direction of the momentum transfer, a measurement of the rocking curves of the film perpendicular to the *c*-direction allows evaluating both its degree of epitaxy and a possible misalignment of the average orientation of its domains with respect to the average orientation of the substrate domains. The relation $d(hkl) = 2\pi/q(hkl)$ is used to calculate the interplanar spacing along the *c*-axes, where $d(hkl)$ is the distance between planes calculated on the base of the (hkl) reflections.

(A) Samples Deposited on Si and on MgO Crystalline Substrates. Using the above formula, the average value of the spacing of the Cr films deposited on Si substrate is (0.900± 0.002) Å, in good agreement with the literature data.

Figure 5 is representative of the films on a Si substrate: the sequence of normalized diffraction patterns of sample 1 collected at various α (keeping the total scattering angle $2\vartheta = 14.85°$ unchanged) is shown. Several diffraction peaks are visible, the one at 6.978(4) Å^{-1} being the [310] reflection of Cr used for the rocking curves computation (shown in the insert). For the films deposited on the MgO substrate, the interplanar spacing along the *c*-axes is (2.037± 0.005) Å, also in accordance with literature values.

In Figure 6, the sequence of normalized diffraction patterns of the film deposited at $T = 500$ °C collected at various α and at fixed $2\vartheta = 9.54°$ is plotted. The diffraction peaks correspond to the [110] reflection of Cr at $q = 3.042(4)$ Å^{-1} and to the [200] reflection of MgO at $q = 2.981(4)$ Å^{-1}, the latter being used for the rocking curve computation. The insert shows the rocking curves relative to the Cr peak.

For all the samples studied, when the α value increases, both the substrate and the film peaks intensity decreases rapidly, showing a very high crystalline quality of the film too. The spectra show that the lattice

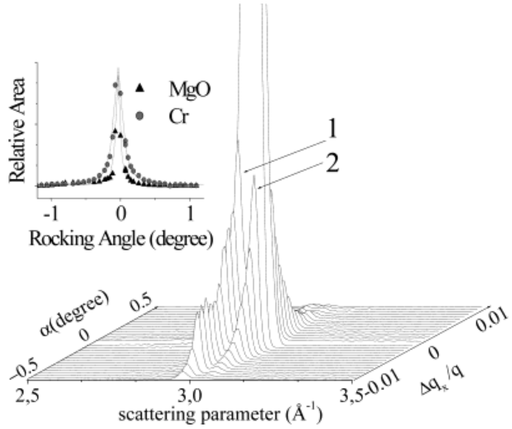

Figure 6. Sequence of the EDXD patterns for the sample no. 8 acquired during the α-scan. The observable reflections are the [200] of MgO at $q = 2.981(4)$ Å^{-1} and the [110] of Cr at $q = 3.042(4)$ Å^{-1}. The insert reports the rocking curve; the relative area of the Cr peak is re-scaled by a factor 10.

structure is very ordered, the growth being perfectly epitaxial along the [310] direction for the films on Si and along the [110] direction for the films on MgO. The result of the rocking curves analysis, reported in Table 1, is that the epitaxy index, estimated as the mean value of fit FWHM, is about (0.050 ± 0.005)° for films deposited on a Si substrate and (0.150 ± 0.005)° for films on a MgO substrate. The (small) fluctuations around the mean value seem not to depend on the film deposition temperature. This indicates that if a correlation exists between this temperature and the mosaic spread of Cr, it produces effects on the epitaxy less than 0.015°.

Concerning the samples deposited on MgO, the substrate and Cr reflections are almost in the same position of the spectrum (see Figure 6), producing only one asymmetric broad peak for all samples except the film deposited at 500 °C, for which the two contributions are sufficiently resolved to perform a complete rocking curves analysis. The sample grown on MgO at a higher substrate temperature, namely, sample 7, shows the presence of an additional peak at $q = 4.365(4)$ Å^{-1} that can be attributed to the [200] reflection of Cr. This contribution is almost irrelevant, as the intensity of this reflection is about 4 orders of magnitude lower than that of the Cr [110] reflection. Nevertheless, as reported in Figure 7, a blowup of the high q region of the diffraction spectra allows following it: from the sequence of the EDXD patterns acquired among the α-scans, though much affected by the background, the FWHM of the reflection is estimated to be about 0.5°. Likely this additional contribution is to be attributed to the presence of a minor fraction of domains not epitaxially oriented. This confirms the hypothesis suggested by the reflectometry measurements on this sample, that is, that in this case the deposition process did not result in a perfectly epitaxial growth. Anyway, the contribution of the domains oriented along the [200] direction appears to be irrelevant to the extent of defining the degree of epitaxy of the films under study: only very accurate and "focused" measurements, together with the combined use of ED reflectometry and diffraction techniques, have evidenced its occurrence.

Finally, the ED technique offers the possibility of gaining diffractometric and spectroscopic data simul-

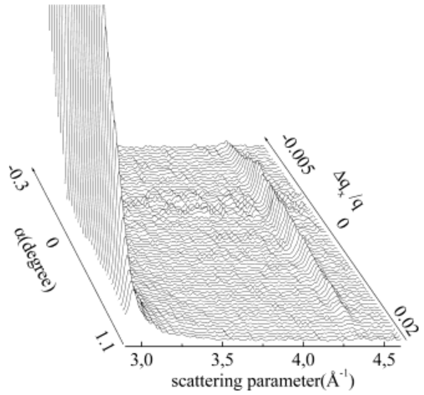

Figure 7. Blowup of the high q region of the diffraction spectra for sample no. 7: sequence of the EDXD patterns acquired during the α-scan. The observable peak at $q = 4.365(4)$ Å^{-1} is the [200] reflection of Cr.

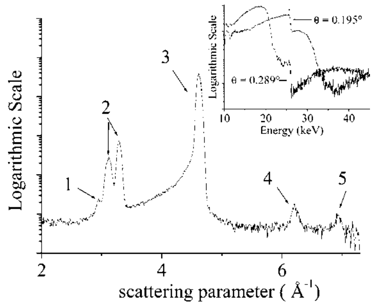

Figure 8. The diffraction spectrum of sample no. 4 shows the evidence of the contamination of the Cr film by Ag. The labeled peaks are as follows: (1) the Kα fluorescence line of Ag; (2) the escape lines of the Ge sensitive crystal associated with peak (3); (3) the [400] reflection of Si; (4) the [220] reflection of Cr; and (5) the [310] reflection of Cr. The reflectometry spectra are strongly affected by the presence of the Ag absorption threshold at about 25 keV, as shown in the insert.

taneously. This characteristic enabled us to detect the presence of a chemical impurity in sample 4. The diffraction spectra (see Figure 8) show, on one side, the evidence of the contamination of the Cr film by Ag (the Ag fluorescence lines are visible), likely due to the presence of silver print on the substrate surface and, on the other side, the spectral markers of a powder diffraction: the [310] reflection is present and the FWHM of its rocking curve is comparable to the one of the other samples, but the [220] reflection is also present and persists when the [310] planes do not reflect any longer. This is indicative of how impurities may compromise epitaxial growth of the films. This picture confirms the results of the reflectometry measurements, reported in the previous paragraph.

(B) Samples Deposited on Amorphous SiO_2 Substrate. The results of the EDXD measurements performed on the Pt/Cr/ SiO_2 films are characterized by the broad hump due to the substrate contribution. In Figure 9 the spectrum acquired at $\alpha = 0.0938°$ is shown: the signal is dominated by the long period of modulation characteristic of the diffractometric response of amorphous SiO_2. Nevertheless, several diffraction peaks are also visible, due to both the Cr and the Pt films. The Cr film experiences oxidation, presumably due to diffusion of the oxygen of the SiO_2 and some peaks of CrO_3 also being present. Moreover, the Cr_3Pt [321] phase has been detected. In particular, two peaks are assigned to the

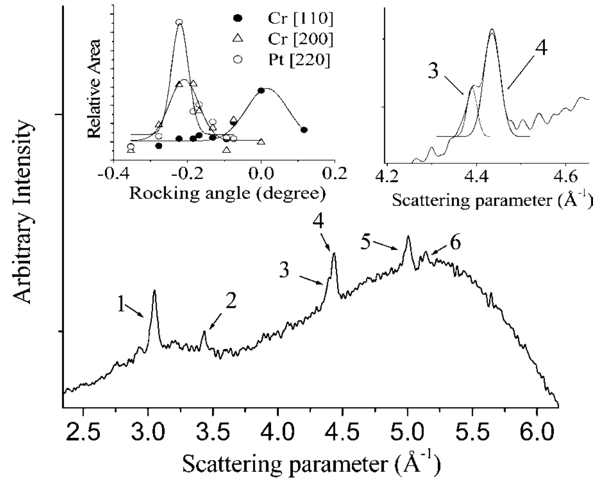

Figure 9. The ED diffraction spectrum (acquired at $\alpha = 0.0938°$) of the Pt/Cr/ SiO_2 sample deposited at RT is shown. The long period of modulation is due to the diffraction response of amorphous SiO_2, while the visible reflections have been indexed as follows: (1) Cr[110] at $q = 3.054(4)$ Å^{-1}, (2) CrO_3-[202] at $q = 3.436(4)$ Å^{-1}, (3) Cr[200] at $q = 4.368(4)$ Å^{-1}, (4) Pt[220] at $q = 4.456(4)$ Å^{-1}, (5) Cr_3Pt[321] at $q = 5.003(4)$ Å^{-1}, and (6) CrO_3[260] at $q = 5.125(4)$ Å^{-1}. The left insert reports the result of the RC analysis for the Cr and Pt reflections. The right insert is a blowup of the central part of the spectrum, showing how the two peaks of Cr[200] and Pt[220] are resolved.

[200] and [110] reflection of the Cr. The rocking curve analysis (see insert of Figure 9) shows that the relative intensity of the two Cr Bragg peaks is comparable; thus, the Cr film growth is not epitaxial. A comparison with the case of films deposited on crystalline substrates can be made, where only the Cr [110] reflection is present. There is one case, namely, for the Pt/Cr/ MgO sample grown at higher substrate temperature, for which the presence of an additional peak attributed to the Cr [200] reflection is visible. However, the RC analysis pointed out that the Cr [110] reflection is in any case largely the dominant contribution and the Cr film growth can be considered epitaxial. On the contrary, when deposition is performed on an amorphous substrate the Cr film does not show any epitaxial growth, in the entire deposition temperature range explored (from RT to 600 °C). Indeed, two reflections of comparable intensity, Cr [110] and Cr [200], are present. The RC analysis shows that the FWHM is of the order of 0.1°.

4. Discussion

All the samples deposited on crystalline (Si and MgO) substrates are grown with a high degree of epitaxy. The maxima of the rocking curves of the Cr film do not coincide with the reference value ($\alpha = 0°$), at which the substrate reflections are most intense, but are slightly misplaced. This can be explained, besides the effect related to a possible miscut of the substrate, by a change of the film orientation with respect to that of the substrate, due to the way the film crystalline lattice matches the substrate lattice. The thickness of the films deduced by EDXR does not seem to be correlated with the widths (FWHM) of the respective rocking curves, which indicates that the substrate−film disorientation is small and random. It can be attributed to the statistical process of depositions. At the energy fluence used in these depositions ($F = 3 \times 10^8$ W/cm^2) the species emitted from the target possess kinetic energy of the order of keV for ions and hundreds of eV for neutrals. This unusually high energy—peculiar to the PLD process at high fluence—favors the epitaxial growth. The mechanism suggested for the initial stages of film growth[17] is the following: the atoms that arrive at the substrate have sufficient energy to cause the formation of individual vacancies in a thin surface layer; subsequently, the vacancies diffuse inside the substrate and recombine within periods on the order of 10^{-8} s without disturbing the crystalline order of the diffusion layer. As a consequence, the superficial layer has a number of vacancies, which greatly exceeds the equilibrium value at a given temperature. The final result is that the adatoms diffusion coefficient on the surface increases proportionally since the adatoms diffusion on a solid occurs mainly at the nonoccupied position of the crystalline lattice. Therefore, the first layers deposited play a key role, imposing the structure to the whole film.

We have compared the results obtained for the films deposited on crystalline substrates, with literature data. In particular, Ishikawa et al.[18] and Shima et al.[19] have deposited Cr layers on a Si substrate by PLD at a fluence of 10 and 7 J/cm^2, respectively. In the first case, Cr layer with no crystalline orientation was obtained, while in the second case, the crystalline oriented Cr layer was obtained only at temperatures higher than 300 °C. In our case, working at lower fluence (5 J/cm^2), we have produced films with high orientation at all the deposition temperatures.

Moreover, the layers we deposited on crystalline substrates showed also a very low roughness of the order of a few Angstroms; this is very important, especially for the magnetorecording application, where the total roughness of the medium must be kept under definite values (between 1.5 and 5 nm).

It is worth pointing out that the results reported show how the combined use of ED reflectometry and diffraction techniques allows correlating an observed unexpected behavior to an effective sample defect: that is, the contamination of the Cr film by Ag impurity in sample 4 and the not perfectly epitaxial growth of sample 7. This is an important tool for excluding the presence of an experimental artifact. Moreover, the PLD technique has been checked as an alternative method for preparing some underlayer with optimized crystalline and morphological properties. Particularly, the samples deposited on crystalline substrates showed a very ordered crystalline structure with a very high degree of epitaxy and the layer showed also very low values of the roughness index, due to the intrinsically high adatom mobility.

Finally, the experimental data showed that the same crystalline and morphological properties can be obtained also by performing the deposition at lower temperature. This result is peculiar of the conditions used to perform the PLD deposition and has recently been obtained also for double-layer CoPt/Cr thin films, to be used as multilayered magnetic media for high-density magnetorecording.[20]

Conclusions

We present a study of Cr/Pt bilayer film by combined energy-dispersive X-ray reflectometry and diffractometry measurements. The former is suitable for morphological characterization of films, while the structural properties are investigated by the latter. In particular, the EDXR technique allows determining the films thickness and roughness and the EDXD gives a straightforward method for the determination of all the Bragg reflections rocking curves.

Comparing the results obtained for the various samples, we observe that when the deposition is performed on a crystalline substrate, epitaxial films with a very good texture and a very smooth surface were obtained. Moreover, no correlation is found between the temperature and the structural and morphological parameters. The conclusion is that when the PLD deposition is performed under controlled working conditions, in particular, with the excimer laser at an energy fluence of 5 J/cm^2, the Pt/Cr multilayer shows a high crystalline quality independent of the deposition temperature. In particular, epitaxial films with strong texture and smooth surfaces, as shown by the very low roughness values, were obtained also when the deposition is carried out at low temperature.

A further benefit of the spectroscopy-based energy-dispersive diffraction technique is the possibility to gain fluorescence data from the sample, allowing detection of the presence of chemical impurities that, in some cases, contaminated the films.

Acknowledgment. This work was supported by the UE Growth program, Project HIDEMAR, Contract No. G5RD-2002-00731. The author wishes to thank Mr. Massimo Brolatti for his constant help in the activity concerning the EDXD and Mr. Daniele Petrelli for technical assistance in PLD films deposition.

CM031100H

(17) Metev, S. In *Pulsed laser deposition of thin films*; Chrisey, D. B., Hubler, G. K., Eds.; John Wiley & Sons: New York, 1994; p 260.
(18) Ishikawa, A.; Tanahashi, K.; Yahisa, Y.; Hosoe, Y.; Shiroishi, Y. *J. Appl. Phys.* **1994**, *75*, 5978.
(19) Shima, M.; Ford, A. C.; Ross, C. A. *IEEE Trans. Magn.* **2000**, *36*, 2321.
(20) Paci, B.; Generosi, A.; Rossi Albertini, V.; Agostinelli, E.; Varvaro, G. *J. Magn. Magn. Mater.* **2004**, in press.